Possibility of Generating a High-Power Self-Similar Radiation Pulse from a Free-Electron Laser

T. B. Zhang and T. C. Marshall
Department of Applied Physics, Columbia University, New York, New York 10027
(Received 5 August 1994)

Using 1D short-wavelength (8 μm) Compton free-electron-laser (FEL) equations with slippage, we explore propagation of a high-power pulse down a tapered undulator FEL traveling-wave amplifier. For an appropriate taper, a short pulse (~300 fsec FWHM) with regular features will propagate self-similarly as it grows in power, slipping through a much longer electron pulse. The power spectrum of the pulse is nearly Gaussian with no sidebands. The electron energy is depressed by ~33%, but slippage causes the peak pulse intensity to be about the same as the electron-beam power density, ~10 TW/cm^2.

PACS numbers: 41.60.Cr, 42.60.Jf

Under certain conditions, the free-electron-laser (FEL) oscillator has been found to provide an output of narrow, chaotic high-power "spike" pulses of radiation characterized by a wide irregular spectrum [1–3]. Furthermore, in the operation of a FEL oscillator, experiment [4] as well as numerical theory which carries the analysis well into the nonlinear regime [5] shows that the FEL can operate in a mode characterized by low efficiency together with a narrow spectrum, or in a mode that has higher efficiency and a wide spectrum. The latter has to do with the sideband instability [6] which has been observed experimentally [7,8] and which is also found in connection with superradiant spiking studies [9–13], since both [14] arise from slippage. However, there is also evidence that the sideband instability can be stabilized with an appropriately chosen taper of the undulator [15–17].

This Letter considers a traveling-wave, high-gain, Compton FEL which operates at nearly optimal efficiency using a variable-parameter undulator and which produces an intense "clean" output spike pulse with a nearly Gaussian spectrum free of sidebands. The hardware would include a laser "seed" source which supplies a high-power pulse having a Gaussian shape, as input to a high-efficiency FEL traveling-wave amplifier having an appropriately tapered undulator. Our findings are that one might expect to develop an infrared FEL pulse having peak power ~10 TW/cm^2 and FWHM ~300 fsec using a 45 MeV, 150 A electron beam. We now develop a numerical model which establishes how such a FEL pulse can be prepared.

We shall study a short optical pulse which is propagating along a much longer pulse of electrons that is traversing an undulator. At FEL resonance, as the light wave moves down one undulator period, it slips ahead of the electrons by one optical wavelength λ_s. We shall study the case where the electron beam pulse is much longer than the overall slippage distance $L_s = N_w\lambda_s$, so that essentially no radiation appears ahead of or behind the electron pulse. (A number of recent publications have considered the wealth of interesting effects which occur at the beginning and the end of the electron pulse, which involve "superradiance" [9–13].) We begin by studying a set of 1D equations which are appropriate for the Compton FEL:

$$\frac{\partial\gamma_j(x,y)}{\partial x} = -\frac{2\rho\gamma_r^2 A_s \sin\psi_j}{\gamma_j\beta_{j\|}}, \tag{1}$$

$$\frac{\partial\theta_j(x,y)}{\partial x} = \frac{1}{2\rho}\left[1 - \frac{k_s(1-\beta_{j\|})}{k_w\beta_{j\|}}\right], \tag{2}$$

$$\frac{\partial A(x,y)}{\partial y} = i\gamma_r\left\langle\frac{e^{-i\theta}}{\gamma}\right\rangle. \tag{3}$$

The above equations are derived directly from the original 1D time-dependent FEL equations [6] by transforming the variables z and t into new independent variables x and y [9], i.e., $x = (ct - z)/l_c$, $y = (z - v_\| t)/l_c\beta_\|$; here, $l_c = \lambda_s/4\pi\rho$ is the cooperation length which is defined as the minimum distance over which an electron may interact cooperatively with the radiation [10], $\rho = \gamma_r^{-1}(a_w\omega_p/4ck_w)^{2/3}$ is the Pierce parameter; $\beta_{j\|} = [1 - (\mu^2 - 2a_w a_s\cos\psi_j)/\gamma_j^2]^{1/2}$ is the axial velocity of the jth electron, $\mu^2 = 1 + a_w^2 + a_s^2$, a_w and a_s are the normalized vector potentials of the undulator ($eB_\perp/k_w mc^2$) and radiation field ($eE_s/k_s mc^2$); γ_j is the relativistic factor of the jth electron, $\psi_j = \theta_j + \phi$ is the relative phase of the jth electron with respect to the radiation pulse, $A(x,y) = A_s e^{i\phi}$ is the complex amplitude of the radiation pulse with $A_s = \omega_s a_s/\sqrt{\gamma_r\rho}\,\omega_p$, and ϕ is the phase shift of the radiation pulse. The angular brackets on the right-hand side of Eq. (3) indicate an ensemble average over all electrons. For the other quantities, γ_r is the resonant energy of electron in units of mc^2, $k_w = 2\pi/l_w$ is the wave number of the undulator, and l_w is the undulator period; $k_s = 2\pi/\lambda_s = \omega_s/c$ is the wave number of the radiation pulse, λ_s is the radiation wavelength, l_w and λ_s satisfy the resonance condition $\lambda_s = l_w(1 + a_w^2)/2\gamma_r^2$, and $\omega_p = (4\pi e^2 n_e/m)^{1/2}$ is the plasma frequency for n_e electrons/cm^3. The original FEL wave equations have been obtained assuming the field amplitude is a slowly varying function of time; this approximation has been

 0031-9007/95/74(6)/916(4)$06.00

verified in the application for the short pulse propagation discussed here.

The numerical simulation is based on the computational model described by Eqs. (1)–(3). The FEL works as a traveling-wave amplifier. The spatial distribution of simulation electrons has a rectangular profile, the electrons are taken to be monoenergetic, and at the undulator entrance, they are uniformly distributed inside the beam length L_b with 1000 simulation electrons per radiation wavelength. For each wavelength-size "strip" of electrons, the relative phase location of the electrons with respect to the radiation field is uniformly distributed from $-\pi$ to π. The input radiation pulse is "seeded" inside the electron beam, with its initial amplitude $a_{s0} = 10^{-4}$ (200 MW/cm^2 at 8 μm wavelength). The pulse profile and width can be varied so that we can study the evolution of various pulses. For the output format of the computational results, the electron-beam pulse and the radiation spike are plotted as the function of independent variables x and y, respectively, which implies two moving "windows" with the former at the speed of light c and the latter at the speed of electrons $v_\parallel$; both are scaled in the units of the radiation wavelength λ_s from their leading edge. Since all these quantities are recorded at various undulator positions, these results will describe the time evolution of the pulses. In several test runs, we have carried out simulations for different FEL parameters, including different lengths of beam pulses and radiation pulses. Our results for superradiant pulse evolution are in a very good agreement with that of previous authors [9] and provide a calibration of our code.

Our main interest is to investigate an initial short radiation pulse propagating through a sufficiently long electron pulse. The initial radiation pulse has a Gaussian profile, shown in Fig. 1(a), and is injected into the rear part of the electron beam pulse; the peak of the initial pulse is located at $x = 225\lambda_s$. The radiation pulse starts from that position at the undulator entrance, and then moves toward the front of the electron pulse as it moves along the undulator. Shown in Fig. 1(b) is the Fourier-transformed spectrum, which has a central frequency $\omega_s = 2.36 \times 10^{14}$ sec^{-1}.

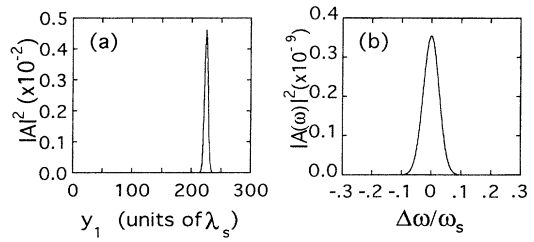

FIG. 1. The initial radiation pulse with a Gaussian profile, shown in (a), upon injection into a rectangular electron beam pulse, $y_1 = \beta_\parallel \ell_c y$. Shown in (b) is the Fourier-transformed spectrum; the central frequency is $\omega_s = 2.36 \times 10^{14}$ sec^{-1} at $\Delta\omega = 0$.

TABLE I. Simulation parameters of radiation spike propagating in electron beam pulse.

Beam parameters	
Electron beam energy	$\gamma = 89.5$
Electron beam current	$I_b = 150$ A
Beam intensity	5.4 TW/cm^2
Electron beam radius	$r_b = 0.02$ cm
Beam pulse length	$L_b = 300\lambda_s$ (2.4 mm)
Undulator parameters	
Undulator period	$l_w = 2.5-1.5$ cm; linear ramp
Undulator taper	$\eta = 2.6 \times 10^{-3}$ cm^{-1}
Undulator parameter	$a_w = 2.0$ (constant)
Undulator length	$N_w = 150$
Radiation pulse	
Radiation wavelength	$\lambda_s = 8.0$ μm
Spike length (FWHM, intensity)	$L_r = 12\lambda_s$
Initial pulse amplitude	$a_{s0} = 10^{-4}$ (200 MW/cm^2)
Peak spike amplitude	$a_s = 0.021$ (9 TW/cm^2)
Other parameters	
Pierce parameter	$\rho = 0.02$
Cooperation length	$l_c = 4.6\lambda_s$

Other simulation parameters of the FEL amplifier are listed in Table I, where a representative electron beam pulse length of 2.4 mm (~8 psec) is taken; the beam pulse is 300 wavelengths long, and so the optical pulse moves only halfway through as it traverses 150 undulator periods.

Figure 2 shows the pulse evolution in a constant period undulator ($l_w = 2.5$ cm). The profiles of electron energy and the radiation spike together with its Fourier-transformed spectrum are shown at two undulator positions $N_w = 75$ [Figs. 2(a1)–2(a3)] and $N_w = 150$ [Figs. 2(b1)–2(b3)]. In these figures, the electron envelope is at rest and the optical spike propagates from the right to left as N_w increases. Figures 2(a2) and 2(b2) show that the optical pulse is amplified while the electron energy is reduced [Figs.2(a1) and 2(b1)]. The "efficiency," defined from the maximum drop in electron energy corresponding to maximum pulse intensity, is ~10%, compared with the efficiency of a steady-state long continuous wave which is ~3%. The radiation spike retains the initial profile until approximately 100 undulator periods where the growth becomes saturated. Saturation occurs when the loss of beam energy causes the interaction to drop out of resonance. A flat region and pulses beside the main spike develop from the two edges of the pulse after it propagates a long distance, and this causes a ragged energy profile [Fig. 2(b1)]. Figure 2(b3) shows a powerful long wavelength sideband comparable in intensity to the carrier; it has about the

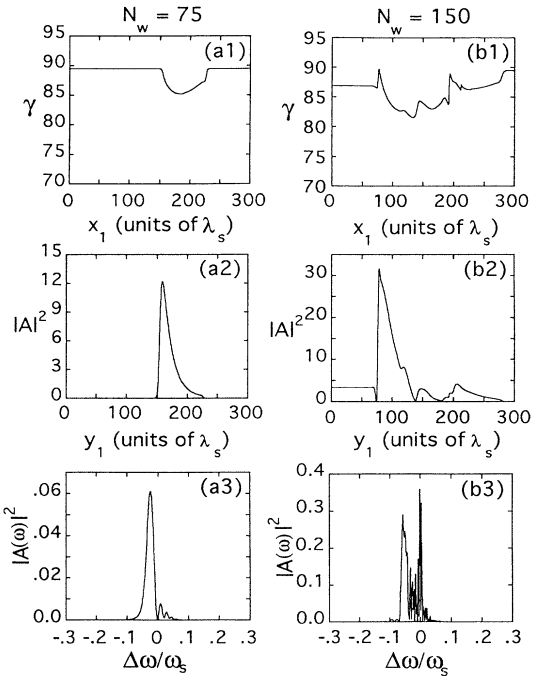

FIG. 2. Constant undulator period simulation. The radiation pulse slips forward into the electron beam from right to left, $x_1 = \ell_c x$. The beam energy distribution, radiation profile, and its Fourier-transformed spectrum (ordinate, arbitrary units) are shown in (a1)–(a3) at $N_w = 75$ and (b1)–(b3) at $N_w = 150$.

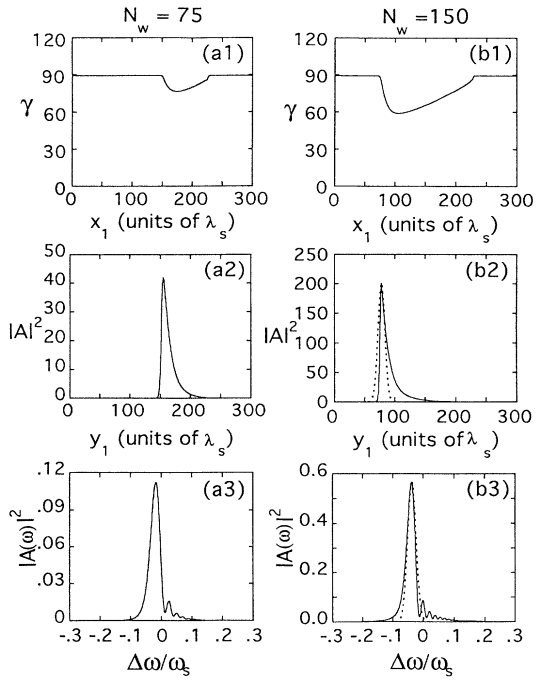

FIG. 3. The parameters are the same as in Fig. 2 except that the undulator period is linearly tapered from 2.5 to 1.5 cm. When the radiation spike slips over the electron beam, the beam energy is continuously extracted (a1) and (b1), while the spike keeps a self-similar profile (a2) and (b2). Its Fourier-transformed spectrum (amplitude in arbitrary units) is shown in (a3) and (b3). A Gaussian comparison pulse (dotted curves), described in the text, is shown in (b2), and its Fourier transform appears in (b3).

same displacement from the carrier [6] as the sideband instability.

If the undulator is tapered, we expect the growth of the sideband can be suppressed, and in Fig. 3 we show the results. The undulator period is linearly tapered from 2.5 to 1.5 cm in 150 periods. All other conditions are the same as in Fig. 2 and are obtained from Table I. In this numerical experiment, we did not optimize the undulator taper to pursue the highest efficiency enhancement: Instead, the appropriate taper was chosen for the purposes of obtaining the cleanest spike (however, this optimized taper is not very different from the taper which extracts maximum energy from the beam). Unlike the untapered cases, the radiation pulse at high amplitude does not radically change its shape, but displays a self-similar profile throughout the slippage region. The width of the initial Gaussian pulse is FWHM $\sim 7\lambda_s$ in intensity; it evolves and becomes broadened to about FWHM $\sim 12\lambda_s$ during the first 50 periods; it continues to grow in amplitude while keeping a nearly constant profile and width. We have tried various widths of the initial Gaussian pulse, as well as a different initial amplitude profile varying as $\sim 1/\cosh(\alpha y)$ (a solitary wave solution [18]), and we find the variation of initial choices converges to a similar output pulse profile and width, although the number of undulator periods needed to form the self-similar pulse profile may vary. This suggests that a short optical pulse may eventually evolve to a self-similar spike in the slippage region of the tapered undulator. The characteristic width of the spike is similar to the prediction of the Ginzburg-Landau solitary wave theory [19]. In the constant period undulator, the self-similar feature is lost when the FEL system goes out of resonance.

We should expect an efficiency enhancement in the tapered undulator. Comparing Fig. 3(b2) with Fig. 2(b2), one finds the efficiency is roughly a factor of 3.3 better than the same FEL with constant-period undulator. The maximum value of the normalized field amplitude $a_s = 0.021$ (~ 9 TW/cm^2) corresponds to an intensity of the same order as the beam kinetic energy intensity; this enhancement in power is caused by the slippage of the radiation pulse over "new" electrons as it moves down the undulator. Now the ragged profile of the electron energy in the constant undulator [Fig. 2(b1)] is found to disappear in the tapered undulator [Fig. 3(b1)]. The strong intensity of the spike forms a very deep potential well which may trap most of electrons even though they have an energy spread. The maximum bucket height $\delta\gamma_{\max}$ may be obtained from $\delta\gamma_{\max}/\gamma_r = 2\sqrt{a_w a_s}/\mu$, which gives the value of $\delta\gamma_{\max} = 10$ at $N_w = 75$

and $\delta\gamma_{\max} = 12.5$ at $N_w = 150$. In this case, it is the undulator taper which helps maintain the resonant wave-particle interaction.

The choice of the 8 μm wavelength was arbitrary although this is representative of FEL performance with the chosen beam parameters. (The same qualitative features were obtained in another tapered undulator FEL simulation for a much lower beam energy and wavelength of 1.5 mm.) Considering diffraction, a Rayleigh range of about one-half the undulator length would require an optical beam larger than the electron-beam diameter we have chosen, or a shorter wavelength. Because of the large optical intensity achieved, one would not expect optical guiding to be effective beyond the region of exponential growth [20].

Finally, the sideband is suppressed in the tapered undulator FEL, as shown in Figs. 3(a3) and 3(b3). In this case, we have a comparatively clean spike in both time and frequency domains. Note also there is a frequency shift from the resonance in these spectra. Frequency shifting is an intrinsic characteristic of the time-dependent FEL equations [21]. We may estimate the frequency shift from the computed phase shift $\phi(x,y) = -i\ \ln(A/A_s)$, and $\Delta\omega/\omega_s = 2\rho\,\partial\phi/\partial x$, obtaining the values of $\Delta\omega/\omega_s = -0.014;\ -0.032$ at the two undulator positions $N_w = 75;\ 150$ which agree approximately with the numerical results. In Fig. 3(b2) is also shown a comparison Gaussian pulse having the same amplitude and FWHM as the self-similar pulse; in Fig. 3(b3) we find the Fourier transform of this comparison pulse (also Gaussian) is a rather good fit to the spectrum of the self-similar pulse. The solitary wave $1/\cosh(\alpha y)$ solution is also very close to the Gaussian fit.

In conclusion, we have found that injection of a single short radiation pulse into a long electron-beam pulse at the input of a tapered undulator traveling-wave FEL amplifier should result in the development of an intense spike which is comparatively clean in both time and frequency domains, and which propagates in a self-similar way along the undulator. Because of the slippage, the peak pulse intensity is enhanced and is of the same order as the electron-beam intensity. Since the pulse spectrum is regular and nearly Gaussian, the output pulse from the FEL is useful for technical applications and indeed might be compressed and intensified even further using standard optical techniques.

This work is sponsored by the Office of Naval Research.

[1] R. W. Warren, J. C. Goldstein, and B. E. Newnam, Nucl. Instrum. Methods Phys. Res., Sect. A **250**, 19 (1986).
[2] B. A. Richman, J. M. J. Madey, and E. Szarmes, Phys. Rev. Lett. **63**, 1682 (1989).
[3] J. W. Dodd and T. C. Marshall, IEEE Trans. Plasma Sci. **PS-18**, 447 (1990).
[4] D. Iracane, V. Fontenay, P. Guimbal, S. Joly, S. Striby, and D. Touati, Phys. Rev. Lett. **72**, 3985 (1994).
[5] D. Iracane and J. L. Ferrier, Phys. Rev. Lett. **66**, 33 (1991).
[6] N. M. Kroll, P. L. Morton, and M. N. Rosenbluth, IEEE J. Quantum Electron. **QE-17**, 1436 (1981).
[7] R. W. Warren, B. E. Newnam, and J. C. Goldstein, IEEE J. Quantum Electron. **QE-21**, 882 (1985).
[8] F. G. Yee, J. Masud, T. C. Marshall, and S. P. Schlesinger, Nucl. Instrum. Methods Phys. Res., Sect. A **259**, 104 (1987).
[9] R. Bonifacio, B. W. J. McNeil, and P. Pierini, Phys. Rev. A **40**, 4467 (1989).
[10] R. Bonifacio, N. Piovella, and B. W. J. McNeil, Phys. Rev. A **44**, 3441 (1991).
[11] W. M. Sharp, W. M. Fawley, S. S. Yu, A. M. Sessler, R. Bonifacio, and L. DeSalvo Souza, Nucl. Instrum. Methods Phys. Res., Sect. A **285**, 217 (1989).
[12] G. T. Moore and N. Piovella, IEEE J. Quantum Electron. **QE-27**, 2522 (1991).
[13] S. J. Hahn and J. K. Lee, Phys. Rev. E **48**, 2162 (1993).
[14] R. M. Caloi, Phys. Rev. A **46**, 7934 (1992).
[15] F. G. Yee, T. C. Marshall, and S. P. Schlesinger, IEEE Trans. Plasma Sci. **PS-16**, 162 (1988).
[16] B. Hafizi, A. Ting, P. Sprangle, and C. M. Tang, Phys. Rev. A **38**, 197 (1988).
[17] R. P. Pila and A. Bhattacharjee, Phys. Plasmas **1**, 390 (1994).
[18] S. Y. Cai and A. Bhattacharjee, Phys. Rev. A **43**, 6934 (1991).
[19] Li-Yi Lin and T. C. Marshall, Phys. Rev. Lett. **70**, 2403 (1993).
[20] E. T. Scharlemann, in *Free Electron Lasers,* edited by W. Colson, C. Pellegrini, and A. Renieri, Laser Handbook Vol. 6 (North Holland, Amsterdam, 1990).
[21] G. Shvets and J. S. Wurtele, Phys. Plasmas **1**, 157 (1994).